Korean J. Chem. Eng., 33(3), 945-951 (2016)
DOI: 10.1007/s11814-015-0251-3

pISSN: 0256-1115
eISSN: 1975-7220

Adsorptive characteristics of the polyurethane-immobilized *Corynebacterium glutamicum* biosorbent for removal of Reactive Yellow 2 from aqueous solution

Sung Wook Won*, Juan Mao, Gopinathan Sankar***, Hyun-Cheol Lee****, and Yeoung-Sang Yun*****,†**

*Department of Marine Environmental Engineering and Institute of Marine Industry, Gyeongsang National University, 38, Cheondaegukchi-gil, Tongyeong, Gyeongnam 53064, Korea
**Department of Environmental Science and Engineering, Huazhong University of Science and Technology, Wuhan 430074, China
***Department of Chemistry, University College London, 20 Gordon Street, London WC1H0AJ, U.K.
****Department of Clinical Pathology, Hanlyo University, 94-13, Hallyeodae-gil, Gwangyang-eup, Gwangyang, Jeonnam 57764, Korea
*****School of Chemical Engineering, Chonbuk National University, Jeonju, Jeonbuk 54898, Korea
(*Received 20 March 2015 • accepted 20 November 2015*)

Abstract−Polyurethane (PU) was evaluated for its possibility as an immobilization matrix for the raw biomass of *Corynebacterium glutamicum*. Initially, different blending ratios of the raw biomass to PU weight were tested, and the ratio of 7 : 3 was identified as the optimal condition. PU-immobilized biosorbent (PUIB) with a particle size ranging from 0.425 to 0.18 mm was selected for the adsorption of Reactive Yellow 2 (RY2). The uptake of RY2 on the PUIB was favorable at acidic pH, especially below 3. According to the Langmuir model, the maximum RY2 uptakes were estimated to be 104.0, 93.3, and 87.3 mg/g at pH 2, 3, and 4, respectively. The pseudo-first-order and pseudo-second-order models were applied to fit the biosorption kinetic data; the latter model fitted the data well with a high coefficient of determination (R^2) and low average percentage error (ε) values. The RY2-sorbed PUIB was able to be regenerated and reused for five cycles of the adsorption and desorption processes.

Keywords: Polyurethane, *Corynebacterium glutamicum,* Reactive Dye, Immobilization, Regeneration

INTRODUCTION

Biosorption has been extensively proposed as a potent alternative for conventional treatment technologies to remove dyes from wastewaters [1]. The exploitation of various biomasses has been widely studied for the same purpose. The capabilities of numerous microorganisms, mainly bacteria and fungi, for the removal of water-soluble dyes have been studied around the world [1-3]. Among them, bacteria have been proven to be a better candidate due to their high sorption performance and comparatively the rapid production of biomass [4]. Our team has previously reported on the inactive bacterial biomasses, which were generated in large quantities as the waste from a fermentation industry, and those were employed for the removal of anionic or cationic dyes in aqueous solutions [5-9]. Especially, the waste biomass of *Corynebacterium glutamicum* has been examined as a biosorbent [7,9]. In previous studies for the removal of reactive or basic dyes, we evaluated the effects of various parameters, such as pH, initial dye concentration, temperature, dye type, and biomass dosage, in batch systems. We found that the maximum uptakes of anionic reactive dyes were exhibited at acidic conditions, whereas those of cationic basic dyes were obtained at alkaline conditions. In the case of industrial scale applications, however, the use of freely-suspended *C. glutamicum* biomass may lead to many problems, such as separation of the suspended biomass from the aqueous medium, intricate handing, and clogging of pipelines and filters.

Bacterial biomass can be immobilized by entrapment technique in polymeric network or attachment to a matrix surface [10]. The first case is that biomass is restrained in the interstices of fibrous or porous materials or in immobilization matrices such as gel or membrane types. Representatively, chitosan and alginate have been used as matrices for the immobilization of biomass. The latter is that the attachment of biomass can occur on the surface of the immobilization matrix by self-adhesion or chemical bonding. Utilizing entrapment or attachment techniques for biomass immobilization appears to be a most promising solution. However, the immobilizing matrix should be mechanically strong and chemically stable against the actual process conditions [11]. Also, the matrix-facilitating diffusion ability of sorbate is of great importance. Natural polysaccharides such as alginate, chitosan, agarose, and carrageenan are commonly used for biomass immobilization [12]. Alginate has received considerable attention because of simple laboratory preparation and its wide use in cell immobilization in biosorption studies [13,14]. However, the major problems of using alginate include its low mechanical strength and tendency to dissolve in alkaline solution, which limit its application under actual effluent treatment conditions. Polyurethane (PU) has been utilized for the immobilization of various microorganisms due to its high

†To whom correspondence should be addressed.
E-mail: ysyun@jbnu.ac.kr

mechanical strength and resistance to organic solvents and microbial attack [15]. PU is an important and versatile class of man-made polymers widely used in the medical, automotive and industrial fields. PU is also known for its easy handling and almost nil toxicity, which validates its potential application in different industries. Besides its xenobiotic origins, PU has been found to be susceptible to natural biodegradation [16]. Thus, the employment of this kind of polymer has proven to be environmentally safe.

This paper reports the possibility of applying PU as a polymer matrix for the immobilization of the waste biomass of *C. glutamicum*. Also, the sorption capacity of a reactive dye, Reactive Yellow 2 (RY2) from aqueous media was evaluated.

MATERIALS AND METHODS

1. Materials

The fermentation waste of the *C. glutamicum* biomass was obtained as a dried powder form from a nucleic acid fermentation industry (Daesang, Gunsan, Korea). The raw biomass (RB) was dried using a spray-drying process for 24 h and immobilized with PU. RY2 as a model reactive dye was purchased from Sigma-Aldrich Korea Ltd. (Yongin, Korea). The general characteristics of RY2 are as follows. It has a color index number of 18972, maximum absorption wavelength (λ_{max}) of 404 nm, dye content of 60-70%, the molecular formula of $C_{25}H_{15}Cl_3N_9Na_3O_{10}S_3$, and the molecular weight of 873.0 g/mol. RY2 exists as a negatively charged ion in aqueous solution since it has three sulfonate groups (Fig. 1). PU was purchased from a local company and nitric acid and sodium hydroxide used in this work were of analytical grade.

2. Preparation of PU-immobilized *C. glutamicum* Biosorbent

Several mixtures of RB and PU were prepared at different mass ratios of 5 : 5, 6 : 4, 6.5 : 3.5 and 7 : 3, respectively. Each mixture of RB and PU was extruded into distilled water and left for 24 h to form solid-type of PU-immobilized *C. glutamicum* biosorbents (PUIBs). In result, the *C. glutamicum* biomass was entrapped in the PU network. The solidified PUIBs with different mass ratios were then separated from the water, washed several times by using distilled water, and dried in an oven at 60 °C for 24 h. The resulting products were referred to as PUIB1 (5 : 5), PUIB2 (6 : 4), PUIB3 (6.5 : 3.5) and PUIB4 (7 : 3). The dried biosorbents were ground and then sieved into four particle size ranges: 0.18-0.425 mm, 0.425-0.6 mm, 0.6-1.0 mm, and >1 mm. Through sorption experiments, PUIB4 with the particle size of 0.18-0.425 mm was selected for evaluating further sorption performance for RY2.

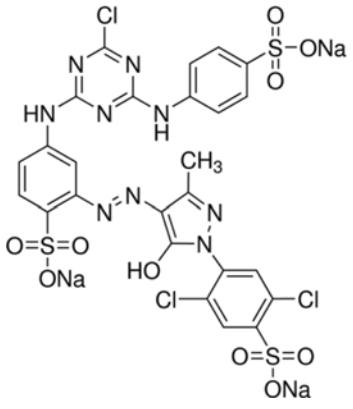

Fig. 1. The chemical structure of Reactive Yellow 2.

3. Biosorption Experiments

Experiments were conducted in 50-mL polypropylene conical tubes at 25 °C as a function of the ratio of RB to PU, particle size, biosorbent dosage, pH, RY2 concentration and contact time. For these experiments, aliquots of 300 and 500 mg/L RY2 solutions were added to each of four conical tubes with 0.1 g in where PU-immobilized biosorbents have different ratios of RB to PU like PUIB1 (5 : 5), PUIB2 (6 : 4), PUIB3 (6.5 : 3.5) and PUIB4 (7 : 3). The tubes were placed on a shaking incubator at 160 rpm for 24 h. After reaching equilibrium, the biosorbents were separated by centrifugation at 3,000 rpm for 5 min. Then the RY2 concentration in the supernatant was determined by using a UV-Vis spectrophotometer (UV-2550, Shimadzu, Kyoto, Japan) at 404 nm after appropriate dilution. To evaluate the effects of particle size and biosorbent dosage, the experiments were performed at 300 mg/L RY2 solution in the same manner as the screening experiments. The particle sizes of PUIB4 used were referred to as >1.0 mm (PUIB41), 1.0-0.6 mm (PUIB42), 0.6-0.425 mm (PUIB43) and 0.425-0.18 mm (PUIB44).

The pH edge experiments involved 300 mg/L of initial RY2 concentration and 2.5 g/L of PUIB44. The pH was initially adjusted and controlled using 0.1 M HNO_3 or 0.1 M NaOH. After 24 h of contact time, the final pH was measured and the samples were taken and centrifuged at 3,000 rpm for 5 min. Isotherm experiments were performed to measure the full saturation capacities of PUIB44 at pH 2, 3 and 4. The concentration of RY2 was varied between 0 and 1,500 mg/L for PUIB44. The remaining procedures were the same as described in pH edge experiments. Kinetic experiments were also conducted at pH 2 under the same experimental conditions described above, except sampling time to determine the attainment of biosorption equilibrium. The experiments mentioned above were carried out in duplicate and the average values were used to describe experimental results.

The dye uptake (Q) was calculated from the difference between the concentrations of RY2 before and after biosorption by using the following equation:

$$Q = \frac{V_0 C_0 - V_f C_f}{M} \quad (1)$$

where C_0 and C_f are the initial and equilibrium RY2 concentrations in the working solution (mg/L), respectively; V_0 and V_f are the initial and final solution volumes (L), respectively; and M is the dry mass of biosorbent (g).

4. Modeling of Isotherms and Kinetics

We attempted to fit the isotherm data to three isotherm models, the Langmuir, Freundlich, and Redlich-Peterson models:

$$\text{Langmuir model: } Q = \frac{Q_{max} b_L C_f}{1 + b_L C_f} \quad (2)$$

$$\text{Freundlich model: } Q = K_F C_f^{1/n_F} \quad (3)$$

$$\text{Redlich-Peterson model: } Q = \frac{K_{RP} C_f}{1 + \alpha_{RP} C_f^{\beta_{RP}}} \quad (4)$$

where Q_{max} is the maximum dye uptake (mg/g); b_L is the Langmuir equilibrium constant (L/mg); K_F is the Freundlich constant ((mg/g) (mg/L)$^{-1/n}$); n_F is the Freundlich constant; K_{RP} is the Redlich-Peterson isotherm constant (L/g); α_{RP} is the Redlich-Peterson isotherm constant (L/mg)$^{1/\beta_{RP}}$; and β_{RP} is the Redlich-Peterson model exponent.

The experimental biosorption kinetic data were modeled by using pseudo-first-order and pseudo-second-order kinetics, which can be represented in their non-linear forms as:

$$\text{Pseudo-first-order model } q_t = q_e(1-\exp(-k_1 t)) \quad (5)$$

$$\text{Pseudo-second-order model } q_t = \frac{q_e^2 k_2 t}{1+q_e k_2 t} \quad (6)$$

where q_e is the amount of dye sorbed at equilibrium (mg/g); q_t is the amount of dye sorbed at time t (mg/g); k_1 is the pseudo-first-order rate constant (L/min); and k_2 is the pseudo-second-order rate constant (g/mg min).

Both isotherm and kinetic data modeling were performed by non-linear regression using Sigma Plot (version 10.0, SPSS, USA) software. The average percentage error (ε) between the experimental and predicted values was calculated using:

$$\varepsilon(\%) = \frac{\sum_{i=1}^{N}(Q_{exp,i} - Q_{cal,i}/Q_{exp,i})}{N} \times 100 \quad (7)$$

where Q_{exp} and Q_{cal} represent the experimental and calculated dye uptake values, respectively, and N is the number of measurements.

5. Repeated Adsorption and Desorption Experiments

The RY2-loaded biosorbent, which was exposed to 300 mg RY2/L at pH 2 and 25 °C, was separated from the biosorbent-water slurry by centrifugation at 3,000 rpm and 5 min. The separated biosorbent was then brought into contact with 40 mL of distilled water adjusted to pH 9 for 6 h in a rotary shaker at 160 rpm. The remaining procedure was the same as that employed in the biosorption equilibrium experiments. After desorption, the biosorbent was washed several times with deionized water, and the regenerated biosorbent was reused for the next biosorption cycle. These cycles of biosorption followed by elution were performed five times to evaluate the feasibility of the biosorbent regeneration.

RESULTS AND DISCUSSION

1. Effects of the Mass Ratio of RB and PU, Particle Size and Sorbent Dosage

The effects of the mass ratio of RB and PU, particle size and biosorbent dosage were investigated in this study. The different blending ratios of RB and PU, such as 5 : 5 (PUIB1), 6 : 4 (PUIB2), 6.5 : 3.5 (PUIB3), and 7 : 3 (PUIB4), were examined at the initial RY2 concentrations of 300 and 500 mg/L. As shown in Fig. 2, the uptake percentage of RY2 increased with the increase in the RB ratio because the RB concentration increased the biosorption capacity of RY2. On the other hand, the only PU without RB did not sorb RY2 (data not shown). It indicates that RB is the sole reason for RY2 biosorption and PU just acting as a carrier or matrix. Compared with the other combination ratios at both RY2 concentrations of 300 and 500 mg/L, the RB : PU ratio of 7 : 3 showed the best results. However, further increasing the RB dosage and reducing the PU percentage could result in a poor mechanical stability. Thus, PUIB4 was selected for further evaluation.

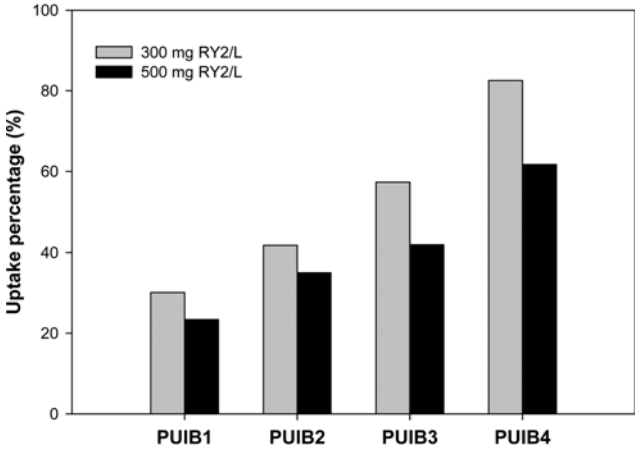

Fig. 2. Screening of four PU-immobilized biosorbents with different ratios of RB and PU (PUIB1: 5 : 5; PUIB2: 6 : 4; PUIB3: 6.5 : 3.5; and PUIB4: 7 : 3).

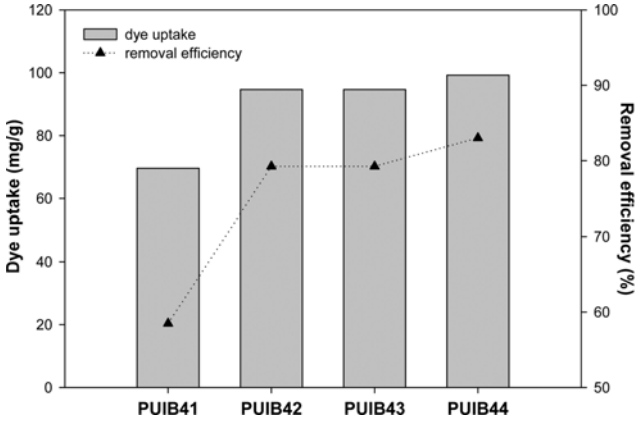

Fig. 3. Effect of particle size on RY2 biosorption by PU-immobilized biosorbent (PUIB41: >1.0 mm; PUIB42: 1.0-0.6 mm; PUIB43: 0.6-0.425 mm; and PUIB44: 0.425-0.18 mm).

The series of PUIB4 were prepared in four different particle sizes (PUIB41: >1.0 mm; PUIB42: 1.0-0.6 mm; PUIB43: 0.6-0.425 mm; and PUIB44: 0.425-0.18 mm). The four particle sizes were tested to identify the appropriate particle size for a better biosorption performance. As seen in Fig. 3, the uptake of RY2 was affected by the particle size of the biosorbents. As the particle size of biosorbent decreased, the dye uptake and the dye removal efficiency were increased from 69.6 mg/g and 58.5% to 99.2 mg/g and 83%. This adsorptive behavior is related to the accessibility of dye molecules to binding sites on the surface of biosorbent. The breaking down of the large particles to make smaller ones can lead to an increase in the surface area and the number of available functional groups of biosorbent. Therefore, the decrease in the particle size of the biosorbent resulted in the enhancement of dye uptake and removal efficiency. Similar observations have been reported by Khataee et al. [17] and Chowdhury and Das [18]. Therefore, the

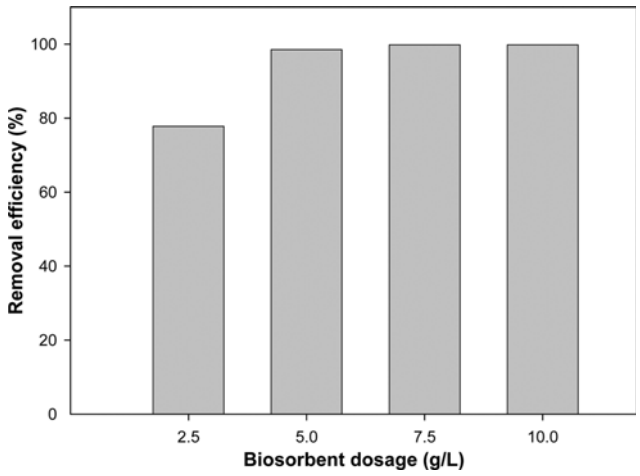

Fig. 4. Effect of biosorbent dosage on RY2 biosorption by PUIB44.

PUIB44 with a particle range of 0.425-0.18 mm was selected for further studies due to its high biosorption capacity.

2. Effect of Biosorbent Dosage

The effect of biosorbent dosage on the RY2 biosorption was studied. As shown in Fig. 4, except for the dosage of 2.5 g/L, all other dosages above 5 g/L showed a similar performance with approximately 100% of removal efficiencies. This result could be attributed to the fact that almost 100% RY2 biosorption had been achieved at 5 g/L and there was no need to increase above 5 g/L of the biosorbent dosage. Thus, a biosorbent dosage of 5 g/L was chosen for all further studies.

3. Effect of Solution pH

The availability of dyes and the activities of the functional groups in the biomass should be affected by the environmental pH. The pH-dependent property of RY2 biosorption onto PUIB44 was estimated by using a pH range of 2.0-11.0 (Fig. 5). The pH effect experiment revealed that the biosorption capacity of RY2 increased with pH decreasing; especially below pH 4, a steep increase in the RY2 uptake was observed. On the other hand, increasing pH beyond 3 resulted in a rapid decrease of the RY2 uptake, and thereafter the biosorption capacity was negligible at pH above 7. Thus, the RY2 biosorption by PUIB44 is optimized to be performed at acidic conditions, whereas an effective desorption is expected at neutral or alkaline conditions.

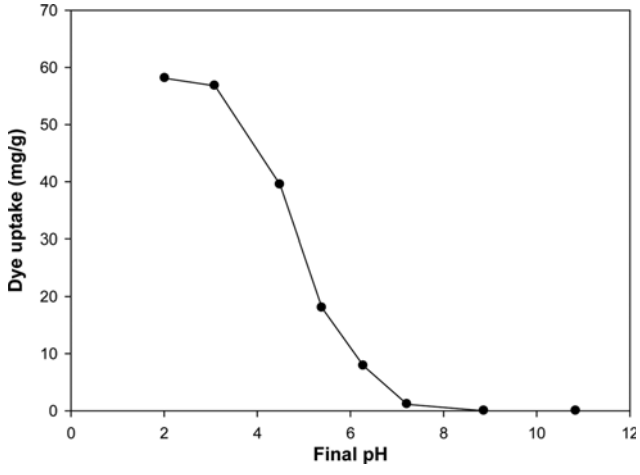

Fig. 5. Effect of pH on RY2 uptake by PUIB44. Experimental conditions: sorbent amount=0.1 g, solution volume=40 mL, initial RY2 concentration=300 mg/L, 25 °C, 24 h, and 160 rpm.

The effect of pH on the RY2 biosorption upon PU-immobilized biosorbent was almost similar to that by freely-suspended raw *C. glutamicum* biomass [19]. This result reflects that the bacterial biomass in the immobilized biosorbent plays a significant role in the binding of RY2. The cell wall of Gram-positive bacterium is mainly comprised of a peptidoglycan layer connected by amino acid bridges [20]. Additionally, the Gram-positive bacterial cell wall consists of polyalcohols, called teichoic acids, which give an overall negative charge to the bacterial cell wall due to the presence of phosphodiester bonds between the teichoic acid monomers [21]. According to our previous report, the *C. glutamicum* biomass is mainly comprised of carboxyl, phosphonate and amine groups [6]. Protonation of the functional groups under acidic conditions results in a net positively-charged biomass. In particular, the negatively-charged amine groups on the surface of *C. glutamicum* were found to be the prime functional groups responsible for the biosorption of reactive dyes [5,6]. Conversely, the reactive dyes release negatively-charged dye ions into solution, which would exhibit electrostatic attraction towards the positively-charged cell surfaces. For this reason, the maximum uptake was shown at acidic conditions. While increasing the solution pH, the carboxyl and phosphonate groups become more negatively charged, which strongly inhibits the binding of anionic reactive dyes to amine groups [22,23].

4. Isothermal Studies

The isotherm experiments were conducted at pH 2, 3, and 4 to assess the maximum biosorption potential of PUIB44. The isotherm results are presented in Fig. 6. The curves showed a sharp increase at lower concentrations and a plateau at higher concentrations, which represented a typical biosorption isotherm curve. The biosorption was higher at lower pH as expected. The isotherms

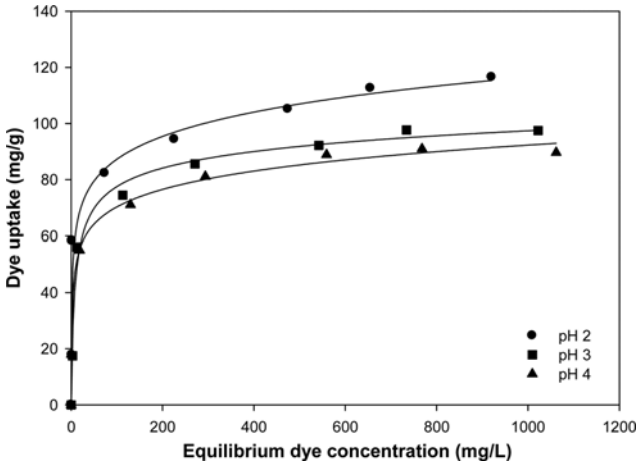

Fig. 6. Biosorption isotherms of PUIB44 at different pH values. Experimental conditions: sorbent amount=0.1 g, solution volume=40 mL, initial RY2 concentration range=0-1,500 mg/L, 25 °C, 24 h, and 160 rpm. Curves predicted by the Redlich-Peterson model.

Table 1. Biosorption isotherm constants obtained from isotherm models

Isotherm models		pH 2	pH 3	pH 4
	Q_{exp} (mg/g)	116.5	97.5	89.7
Langmuir	Q_{max} (mg/g)	104.0	93.3	87.3
	b_L (L/mg)	0.348	0.094	0.094
	R^2	0.911	0.977	0.964
	ε (%)	10.0	2.02	9.41
Freundlich	K_F (L/g)	37.0	28.3	30.0
	n_F	5.85	5.33	5.97
	R^2	0.942	0.949	0.975
	ε (%)	12.4	10.4	6.07
Redlich-Peterson	K_{RP}	77.3	12.6	47.2
	α_{RP}	1.53	0.21	1.11
	β_{RP}	0.879	0.925	0.887
	R^2	0.950	0.988	0.997
	ε (%)	9.86	3.75	0.02

were steep, thus indicating the high affinity of the sorbate towards the biosorbent.

The isotherm data was attempted to be modeled using a two-parameter model such as the Langmuir and Freundlich models and a three-parameter model, the Redlich-Peterson model, to represent the non-linear equilibrium relationships between the amount of sorbed sorbate on the sorbent and the sorbate remaining in solution at constant temperature. The model constants along with the coefficient of determination (R^2) and average percentage error (ε) values obtained from the three isotherm models are listed in Table 1.

The Langmuir isotherm model has been frequently applied to quantify and contrast the sorption performance of different sorbents. It assumes that the sorption occurs at specific homogeneous sites within the sorbent. The utilization of the Langmuir model was extended to empirically depict equilibrium relationships between the liquid and solid phases [24]. According to the simulation of the Langmuir model, the maximum uptakes of PUIB44 were estimated to be 104.0, 93.3, and 87.3 mg/g at pH 2, 3, and 4, respectively (Table 1). However, compared to our previous study [19], the Q_{max} of PUIB44 (104.0 mg/g) at pH 2 was lower than that of raw *C. glutamicum* biomass (154.3 mg/g). It indicates that the immobilization of raw biomass with PU leads to a decrease in dye adsorption capacity. The Langmuir constant b_L indicates the affinity between the sorbent and sorbate. The values of b_L were increased as pH decreased from 4 to 2. The high values of b_L are reflected in the steep initial slope of a sorption isotherm, thereby indicating a desirable high affinity. In general, high Q_{max} and b_L are desirable for good biosorbents.

The Freundlich isotherm was originally empirical, but it was later interpreted as sorption to heterogeneous surfaces or surfaces supporting sites of varied affinities. At all pH values, the isotherm data was well fitted with high R^2 values (>0.94). As given in Table 1, the Freundlich constant K_F reached its corresponding maximum value at pH 2. This result means that the binding capacity reached the highest value compared to the other conditions investigated. The Freundlich constant n_F values were in the range of 1-10, thus indicating that the biosorption of RY2 on PUIB44 was favorable within the performed conditions.

To improve the fitness of the experimental isotherm data, a three-parameter model, the Redlich-Peterson isotherm, was used. This model incorporated the features of the Langmuir and Freundlich isotherms with the mechanism of biosorption being a hybrid. Compared to the other two-parameter models, the Redlich-Peterson model well described RY2 biosorption data with the higher coefficient of determination (R^2) and lower percentage error (ε) values. Regression results are shown in Table 1. The exponent (β_{RP}) values were in the range of 0.879-0.925 at different pHs from 2 to 4. There are two limiting behaviors: Langmuir form for β_{RP}=1 and Henry's law form for β_{RP}=0 [25]. The values of β_{RP} were close to the unity, indicating that the isotherm data can be preferably fitted with the Langmuir model. However, the isotherm data cannot be assumed to be of complete Langmuir form. The K_{RP} values indicated that the RY2 adsorption capacity of PUIB41 was maximized at pH 2 in pH ranges (2-4) examined in this work. This result was consistent in those predicted by the Langmuir and Freundlich models. Generally, the three-parameter models well explain the biosorption isotherm data compared to the two-parameter models as this present study is shown.

5. Kinetic Studies

The sorption kinetics in wastewater treatment is significant as it provides valuable insights into the reaction pathways and into the mechanism of sorption reactions. Also, the kinetics describes the solute uptake, which in turn controls the residence time of the sorbate uptake at the solid-solution interface [26]. The kinetic experiments were carried out at two different initial RY2 concentrations of 300 and 500 mg/L, respectively. Fig. 7 depicts the effect of the contact time on the RY2 biosorption on PUIB44. The uptake of RY2 by PUIB44 was dependent on the initial dye concentration, and the higher RY2 uptake was observed at higher initial dye concentration. However, the removal efficiency of RY2 slightly decreased

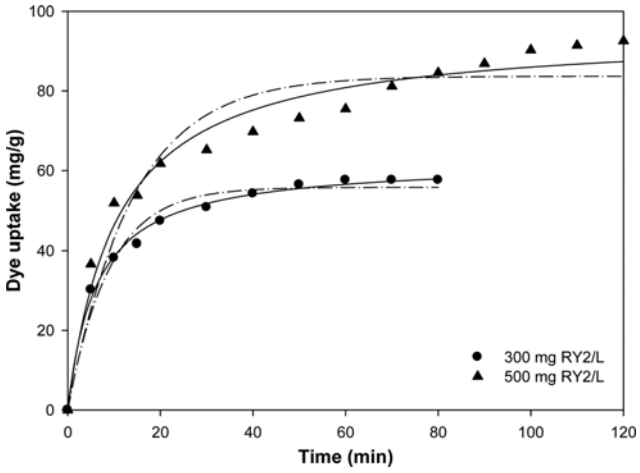

Fig. 7. Biosorption kinetics of PUIB44. Experimental conditions: sorbent amount=0.1 g, solution volume=40 mL, initial RY2 concentrations=300 and 500 mg/L, 25 °C, and 160 rpm. Curves were predicted by pseudo-first-order (dash-dot line) and pseudo-second-order (solid line) models.

from 98.1% to 95.4% as the RY2 concentration increased from 300 to 500 mg/L. This result may have occurred because at lower concentrations, the amount of the initial dye molecules available on the biosorbent surface is less than that of the binding sites in the immobilized biosorbent. Thus, the fractional biosorption becomes independent of the initial dye concentration. On the other hand, the more dye molecules that exist, then the more intense competition with binding sites available for RY2 at higher concentrations occurs. Hence, the removal percentage of RY2 is dependent upon the initial dye concentration. As seen from Fig. 7, in terms of the initial RY2 concentration of 300 mg/L, the maximum sorption capacity (approximately 95% of total amount of RY2 removed) of RY2 was obtained within the first 40 min, and thereafter, the biosorption rate tended to decrease and proceeded at a slower rate. A similar trend was also observed in the kinetic experiments with the initial RY2 concentration of 500 mg/L. The initial rapid phase may be due to the number of vacant sites available at the initial stage. As a result, the concentration gradient between the sorbate in the solution and the sorbate in the biosorbent increased [27]. Equilibrium time was attained at 60 min for the biosorption studies with the initial concentration of 300 mg/L, whereas it was above 120 min for the initial concentration of 500 mg/L. The equilibrium time is a significant factor for the design of pollutant treatment systems since it affects reactor size and plant economics [28].

The experimental biosorption kinetic data were fitted using non-linear pseudo-first-order and pseudo-second-order kinetics. The rate constants, the predicted equilibrium uptakes, and the R^2 values for the dye concentrations tested have been estimated and summarized in Table 2. In the case of the pseudo-first-order model, the R^2 values were 0.973 and 0.919 for initial RY2 concentrations of 300 and 500 mg/L, respectively. However, the calculated Q_e was not close to the experimental Q_e, which suggests that the pseudo-first-order model is not suitable to fit the kinetic experimental data. The reason for these differences between the experimental and calculated Q_e values may be due to a time lag and/or a boundary layer or an external resistance controlling at the beginning of the sorption process [29]. As reported in most literature, the pseudo-first-order model did not fit the kinetic data well for the whole range of contact time and generally underestimated the Q_e values [28,30].

Table 2. Biosorption kinetic constants obtained from pseudo-first-order and pseudo-second-order models

Kinetic models		300 mg/L	500 mg/L
	q_{exp} (mg/g)	57.6	92.6
Pseudo-first-order	q_e (mg/g)	55.8	83.7
	k_1 (L/min)	0.112	0.072
	R^2	0.973	0.919
	ε (%)	0.086	0.354
Pseudo-second-order	q_e (mg/g)	62.4	95.1
	k_2 (g/mg min)	0.003	0.001
	R^2	0.995	0.970
	ε (%)	0.038	0.002

The pseudo-second-order model is based on the sorption capacity on the solid phase. Compared to the pseudo-first-order model, it predicted the sorption behavior over the whole range of studies and was in agreement with a chemisorption mechanism being the rate-controlling step [29]. As shown in Table 2, the results generated from the pseudo-second-order model corresponded with the experimental data with the high R^2 values. The R^2 values obtained by the pseudo-second-order model were greater, and the average percentage error (ε) values were lower than those values for the pseudo-first-order model. Therefore, the pseudo-second-order model can be used to describe the kinetic data of the PU-immobilized biosorbent.

6. Repeated Adsorption and Desorption

If the biosorption process could be employed as an alternative technique in the wastewater treatment scheme, then regeneration of the biosorbent is crucial for keeping the process costs down and opening the possibility of recovering dye molecules extracted from the liquid phase [31]. For this purpose, it is desirable to desorb the sorbed dye and to regenerate the exhausted biosorbent for application of another cycle. According to the results of pH edge experiments, RY2 could not adsorbed onto the biosorbent at above pH 7. Thus, desorption was attempted at pH 9, and the PU-immobilized biosorbent after desorption was tried for the next biosorption cycle at pH 2. We repeated five cycles of adsorption/desorption processes to identify the possibility of the regeneration of the PU-immobilized biosorbent. As seen in Fig. 8, repeating the five cycles of adsorption/desorption processes revealed that there was not any significant difference in either the biosorption efficiency or the desorption efficiency during five cycles. The biosorption efficiency decreased less than 5% until the fifth cycle, which validated the regeneration ability of PUIB in future industrial applications.

CONCLUSIONS

Considering the practical difficulties in handling RB powder in real treatment processes, the immobilization of RB with a proper

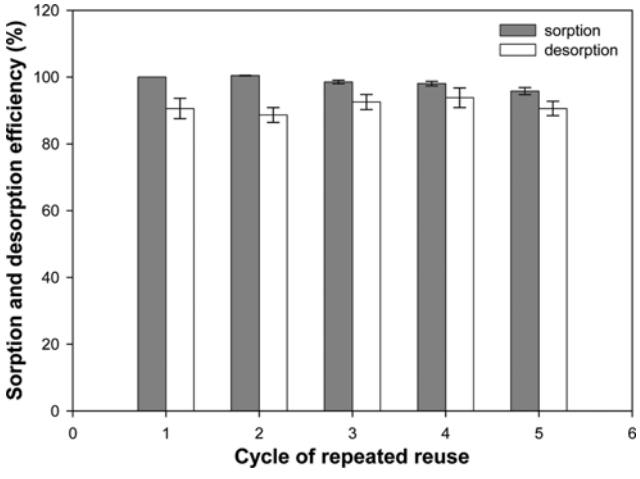

Fig. 8. Regeneration and reuse of PUIB44 in five cycles of sorption/desorption processes. Sorption was performed at pH 2 while desorption was carried out at pH 9.

matrix material like PU was developed. The 7 : 3 mass ratio of RB : PU was found to be optimal, and the PU-immobilized biomass with the range of particle size 0.425-0.18 mm showed the best RY2 biosorption performance. The biosorbent dosage of 5 g/L was also found to be the optimal condition. The solution pH values largely influenced the sorption capacity of PUIB44, and the biosorbent performed well for the RY2 biosorption at pH 2. The maximum uptake at pH 2 was estimated to be 104.0 mg/g using the Langmuir model. The study on the biosorption kinetics using pseudo-first-order and pseudo-second-order models demonstrated that the pseudo-second-order model fitted the kinetic data well with high R^2 and low ε values. The regeneration experimental results at pH 9 revealed that the PUIB44 exhibited invariable RY2 biosorption capacity with a very high mechanical stability even at the end of fifth cycle, thus confirming the technical feasibility of using a PU-immobilized biosorbent in industrial applications. Therefore, PU showed desirable properties for bacterial biomass immobilization and may have potential use in process applications due to its relatively high biomass loading, good chemical and physical stabilities.

ACKNOWLEDGEMENTS

This work (RPP-2013-1028) was supported by the fund of Research Promotion Program, Gyeongsang National University, 2013. This study was partially supported by the international collaborative research funds of Chonbuk National University, 2011.

REFERENCES

1. A. Srinivasan and T. Viraraghavan, *J. Environ. Manage.*, **91**, 1915 (2010).
2. K. Vijayaraghavan and Y.-S. Yun, *Biotechnol. Adv.*, **26**, 266 (2008).
3. P. Kaushik and A. Malik, *Environ. Int.*, **35**, 127 (2009).
4. J. Wang and C. Chen, *Biotechnol. Adv.*, **27**, 195 (2009).
5. S. W. Won, H.-J. Kim, S.-H. Choi, B.-W. Chung, K.-J. Kim and Y.-S. Yun, *Chem. Eng. J.*, **121**, 37 (2006).
6. S. W. Won, S. B. Choi and Y.-S. Yun, *Colloid Surf., A-Physicochem. Eng. Asp.*, **262**, 175 (2005).
7. K. Vijayaraghavan and Y.-S. Yun, *J. Hazard. Mater.*, **141**, 45 (2007).
8. K. Vijayaraghavan, S. W. Won, J. Mao and Y.-S. Yun, *Chem. Eng. J.*, **145**, 1 (2008).
9. J. Mao, S. W. Won, J. Min and Y.-S. Yun, *Korean J. Chem. Eng.*, **25**, 1060 (2008).
10. A. C. Jen, M. C. Wake and A. G. Mikos, *Biotechnol. Bioeng.*, **50**, 357 (1996).
11. S. D. Kumar, P. Santhanam, R. Nandakumar, S. Ananth, B. Balaji Prasath, A. Shenbaga Devi, S. Jeyanthi, T. Jayalakshmi and P. Ananthi, *Afr. J. Biotechnol.*, **13**, 2288 (2014).
12. S. R. Couto, *Biotechnol. Adv.*, **27**, 227 (2009).
13. V. V. Panić, S. I. Šešlija, A. R. Nešić and S. J. Veličković, *Hem. Ind.*, **67**, 881 (2013).
14. O. Prodanovic, D. Spasojevic, M. Prokopijevic, K. Radotic, N. Markovic, M. Blazic and R. Prodanovic, *React. Funct. Polym.*, **93**, 77 (2015).
15. M. F. Silva, D. Rigo, V. Mossi, R. M. Dallago, P. Henrick, G. O. Kuhn, C. D. Rosa, D. Oliveira, J. V. Oliveira and H. Treichel, *Food Bioprod. Process.*, **91**, 54 (2013).
16. G. T. Howard, *Int. Biodeterior. Biodegrad.*, **49**, 245 (2002).
17. A. R. Khataee, F. Vafaei and M. Jannatkhah, *Int. Biodeterior. Biodegrad.*, **83**, 33 (2013).
18. S. Chowdhury and P. Das, *Environ. Prog. Sustain. Energy*, **31**, 415 (2011).
19. S. W. Won and Y.-S. Yun, *Dyes Pigm.*, **76**, 502 (2008).
20. M. U. Mera, M. Kemper, R. Doyle and T. J. Beveridge, *Appl. Environ. Mircobiol.*, **58**, 3837 (1992).
21. N. G. Ravichandra, *Fundamentals of plant pathology*, PHI Learning, Delhi (2013).
22. J. Cai, L. Cui, Y. Wang and C. Liu, *J. Environ. Sci.*, **21**, 534 (2009).
23. J.-F. Gao, J.-H. Wang, C. Yang, S.-Y. Wang and Y.-Z. Peng, *Chem. Eng. J.*, **171**, 967 (2011).
24. T. A. Davis, B. Volesky and A. Mucci, *Water Res.*, **37**, 4311 (2003).
25. Y. S. Ho, C. T. Huang and H. W. Huang, *Proc. Biochem.*, **37**, 1421 (2002).
26. Q. Zhou, Y. Duan, C. Zhu, J. Zhang, M. She, H. Wei and Y. Hong, *Korean J. Chem. Eng.*, **32**, 1405 (2015).
27. M. R. Fat'hi, A. Asfaram, A. Hadipour and M. Roosta, *J. Environ. Health Sci. Eng.*, **12**, 62 (2014).
28. K. S. Thangamani, M. Sathishkumar, Y. Sameena, N. Vennilamani, K. Kadirvelu, S. Pattabhi and S. E. Yun, *Bioresour. Technol.*, **98**, 1265 (2007).
29. G. McKay, Y. S. Ho and J. C. Y. Ng, *Sep. Purif. Methods*, **28**, 87 (1999).
30. M. Sathishkumar, A. R. Binupriya, D. Kavitha and S. E. Yun, *Bioresour. Technol.*, **98**, 866 (2007).
31. B. Volesky, *Hydrometallurgy*, **59**, 203 (2001).